

Informational approach to cosmological parameter estimation

Michelle Stephens,^{*} Sara Vannah,[†] and Marcelo Gleiser[‡]

*Department of Physics and Astronomy
Dartmouth College, Hanover,
New Hampshire 03755, USA*

(Dated: November 24, 2020)

We introduce a new approach for cosmological parameter estimation based on the information-theoretical Jensen-Shannon divergence (\mathcal{D}_{JS}), calculating it for models in the restricted parameter space $\{H_0, w_0, w_a\}$, where H_0 is the value of the Hubble constant today, and w_0 and w_a are dark energy parameters, with the other parameters held fixed at their best-fit values from the Planck 2018 data. As an application, we investigate the H_0 tension between the Planck temperature power spectrum data (TT) and the local astronomical data by comparing the Λ CDM model with the w CDM and the $w_0 w_a$ CDM dynamic dark energy models. We find agreement with other works using the standard Bayesian inference for parameter estimation; in addition, we show that while the \mathcal{D}_{JS} is equally minimized for both values of H_0 along the (w_0, w_a) plane, the lines of degeneracy are different for each value of H_0 . This allows for distinguishing between the two, once the value of either w_0 or w_a is known.

INTRODUCTION

The concordance cosmological model, Λ CDM, is in excellent agreement with data spanning a broad range of redshifts, including the temperature anisotropies of the cosmic microwave background (CMB) [1], the large-scale galaxy clustering feature of baryon acoustic oscillations (BAO) [2], and the luminosity-redshift relation of local sources, calibrated primarily with type-Ia supernovae data (SNeIa) [3]. The model has six independent parameters, assuming the dark energy (DE) equation of state is a constant $w = -1$, and a flat universe: the amplitude and spectral index of the primordial density perturbations, A_s and n_s , respectively; the reionization optical depth τ ; the present-day Hubble parameter H_0 ; and the present-day physical baryon and dark matter densities $\Omega_b h^2$ and $\Omega_c h^2$, respectively, where $h = H_0/100$.

The Friedmann equation for a spatially flat universe with a cosmological constant Λ , in the matter-dominated era ($z \ll 3200$) can be written as $\Omega_b + \Omega_c + \Omega_\Lambda = 1$, where H_0 determines the critical density normalization on Ω_X . Thus, the cosmic expansion history and structure formation in the universe is sensitive to the relative contributions of $\Omega_m = \Omega_b + \Omega_c$, and DE. Despite the overall success of Λ CDM, statistically significant tensions exist between early-universe parameter inference and direct local measurement, most notably in the value of the Hubble parameter today, H_0 [4–6]. Recent results indicate that the discrepancy does not appear to be dependent on the use of any one method of measuring H_0 in the late universe, yielding a persistent tension with early-universe measurements between 4.0σ and 5.8σ [7].

Measurements of the CMB anisotropies at $z \approx 1100$ by the Planck [8] and WMAP [9] missions constrain the combinations $\Omega_b h^2$ and $\Omega_c h^2$, but degeneracies prevent constraints of H_0 alone [10–12]. Local measurements can probe $H(z)$ directly through the luminosity-redshift relation, but distances to sources must be carefully calibrated to avoid systematic error. Uncertainties have been re-

duced to the subpercent level in the case of the Planck analysis, and to the 1% level with recent advances in the local distance-ladder determinations [13, 14]. Excluding an as-yet unknown source of error in either of these analyses, the discrepancy may point to new early-universe physics beyond the standard cosmological model.

Several possible resolutions to the Hubble tension have been proposed, including evolving DE with a phantom-like equation of state [15], additional neutrinos [16, 17], local voids [18], and prerecombination modifications to DE (early dark energy) [19], among many others [17, 20–22]. Given the many data sets, extending the cosmological parameter space and performing a Markov chain Monte Carlo (MCMC) analysis to determine the most likely parameters is a computationally expensive problem [23] and involves many complications in constructing the likelihood function arising from particular instrumentation, data-set considerations, and prior choices [24–26].

Here, we propose an alternative approach to cosmological parameter estimation based on a measure from information theory known as the Jensen-Shannon divergence (\mathcal{D}_{JS}). We apply it to a one-parameter extension of the Λ CDM model, the (w_0, w_a) parametrization of an evolving dark energy component. In Sec. II, we review the standard maximum likelihood method before introducing the \mathcal{D}_{JS} and the information theory needed for its interpretation, with a toy example. In Section III, we provide motivation for using the \mathcal{D}_{JS} to examine linearly evolving DE models and detail the numerical approach. Results are presented in Sec. IV. In Sec. V, we highlight prospects for extending this study in future work.

PARAMETER ESTIMATION

Maximum likelihood estimation

The standard approach for cosmological parameter estimation is a problem of Bayesian inference: We begin

with a data set D , which we wish to accurately represent with a model parametrized by θ . We assume a prior distribution over the parameters, $p(\theta)$. The prior ideally represents our best knowledge of the parameters, but in practice, it is commonly taken to be uniform. The model is specified by the form of the likelihood function, $\mathcal{L}(\theta) \equiv p(D|\theta)$ —the probability that the data are observed, given the model. The posterior probability $p(\theta|D)$ is, by Bayes’ rule, proportional to $p(D|\theta)p(\theta)$. The best parameters are inferred by maximizing the likelihood function.

Details of this method applied to cosmology can be found in Refs. [27–29]. The MCMC code COSMOMC [30] can incorporate the likelihoods for various data sets as well as prior specifications; it is well validated and the most commonly used code for cosmological parameter estimation. In this work, we allow w_0 and w_a to vary while setting H_0 to its value first from early-universe parameter inference and then from local direct measurement. In future work we will extend the analysis using \mathcal{D}_{JS} to the full parameter space. Parameter estimates with confidence intervals can then be directly compared to maximum likelihood results.

Jensen-Shannon divergence

Shannon’s seminal paper [31] provides the foundation for the definition and interpretation of the \mathcal{D}_{JS} . We typically think of describing a message or event in terms of a distinct encoding scheme—a set of symbols $\mathcal{N} = n_1, n_2, \dots, n_L$. For instance, in English we encode words with the 26 letters of the alphabet, and full messages with additional characters for punctuation. The information content of a particular symbol is $I(n) = -\log_2 p(n)$, where $p(n)$ is the probability distribution over symbols in \mathcal{N} determined from some collection of events encoded by \mathcal{N} . The expected value of information in a particular event is then

$$\langle I \rangle = - \sum_{n \in \mathcal{N}} p(n) \log_2 p(n). \quad (1)$$

The \mathcal{D}_{JS} is a measure of the difference between two probability distributions, based on the Kullback-Leibler divergence (DKL) between two distributions $p(n)$ and $q(n)$, defined as [32]

$$\mathcal{D}_{\text{KL}}(p \parallel q) = \sum_n p_n \log \left(\frac{p_n}{q_n} \right). \quad (2)$$

If q is treated as a model for some “true” distribution p , DKL is a measure of the information lost in using q rather than p . DKL is positive-definite, and it is zero only if the two distributions are the same (known as the identity of indiscernibles). However, it is not symmetric

and does not satisfy the triangle inequality: while we picture it as a “distance” between two distributions, it is not a metric. The \mathcal{D}_{JS} is a symmetrized extension of DKL that can be treated as a true metric on the space of probability distributions [33]. It is defined as

$$\mathcal{D}_{\text{JS}} = \frac{1}{2} \mathcal{D}_{\text{KL}}(p \parallel r) + \frac{1}{2} \mathcal{D}_{\text{KL}}(q \parallel r), \quad (3)$$

where $r = \frac{1}{2}(p + q)$. Here, $0 \leq \mathcal{D}_{\text{JS}} \leq 1$ if the logarithm used in the DKL is base 2. In this case, information is measured in bits. With the exception of the next example, we use the natural logarithm, so that $0 \leq \mathcal{D}_{\text{JS}} \leq \ln(2)$.

As a simple illustration of the \mathcal{D}_{JS} , consider a collection of short messages in English. Suppose we eliminate the spaces, capitalization, punctuation, etc., so that the set of symbols from which each message is drawn is simply the 26-character English alphabet. Using the \mathcal{D}_{JS} , we can find out how well each of these messages models the phrase “Cosmology Rocks.”

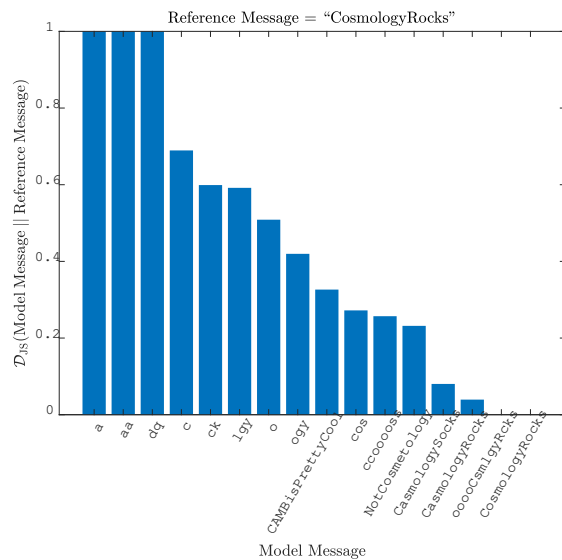


FIG. 1. \mathcal{D}_{JS} between the model messages and the reference message is shown, where the messages are case insensitive and drawn from the English alphabet of 26 letters. This illustrates that the \mathcal{D}_{JS} is sensitive only to the identity and relative frequencies of letters in a message. It is maximal for distributions with nothing in common and minimal (at zero) for identical distributions.

It is clear that only the relative *frequency* of letters in each of the phrases determines the \mathcal{D}_{JS} to the reference message—variables such as ordering of the letters and overall length are irrelevant. Model messages in which none of the letters appears in the reference message are maximally divergent, and those which letter frequencies close to the reference message have low divergence. These results are shown in Fig. 1.

The more interesting examples come from compar-

ing the \mathcal{D}_{JS} for model messages like “lgy,” “cos,” and “ccoooooss.” In the first model, the entire message appears in the reference with the appropriate letter frequency. In the second, the model is comprised of the three most common letters from the reference but with incorrect frequencies. In the final model, the most common letters from the reference appear with the correct frequency. We conclude, then, that the \mathcal{D}_{JS} is sensitive to the most salient features of a given distribution.

It is this property that makes it a good candidate for examining the divergence between the measured angular power spectrum of the microwave background and a model’s prediction for it. If we replace the alphabet with the multipole moment l , and the frequency with C_l , it is the location and relative scaling of the acoustic peaks that provides the bulk of the CMB’s sensitivity to cosmological parameters. Finally, we note that if $q_n = p_n \pm \delta p_n$, with $\delta p_n \ll p_n$, expanding the \mathcal{D}_{JS} to first order in δp_n gives a measure proportional to the chi square.

METHODS

Dark energy and the H_0 tension

The H_0 tension can be stated in this way: late-time scale factor expansion is occurring faster than we would expect from Λ CDM, with parameter constraints inferred from early-universe data. Framed this way, it is easy to see why most of the proposed resolutions involve modifying DE in some way. Prerecombination modifications to DE can alter the sound horizon r_s and thus change the inferred H_0 , while minute shifts in other parameters maintain the agreement with CMB anisotropies [19]. Late-time modifications are an obvious mechanism to alter the expansion history and galaxy clustering, but are constrained by other measurements, notably BAO [34–36]. Constraining the DE equation of state is challenging, because density parameters and $H(z)$ are sensitive to a function of its integral over redshift.

Observational surveys like the DESI probe [37] will be able to provide direct constraints on $w(z)$. Until then, phenomenological models have been introduced to capture what the general behavior of $w \neq -1$ might look like, and its influence on cosmological observables. A common parametrization for evolving DE is the linear evolution model $w = w_0 + w_a(1 - a)$, where w_0 is the value today and $w_a = -dw/da$ [38]. In this framework, Λ CDM corresponds to $w_0 = -1, w_a = 0$, and other constant- w models can be considered by setting $w_a = 0$.

Several studies have extended the Λ CDM basic six-parameter model to include these parameters, constraining them in the extended space via standard MCMC max-likelihood methods. References [15, 23, 39, 40] are an incomplete list.

Data and numerical approach

We compare a model’s prediction for the angular power spectrum to the Planck 2018 data by computing $\mathcal{D}_{\text{JS}}(F_l^{\text{mod}} || F_l^{\text{plk}})$ as in Eq. (3), where F_l^{mod} and F_l^{plk} are determined from the model-predicted and Planck data-calculated angular power spectra, respectively. That is,

$$F_l = \frac{D_l}{\sum_l D_l}, \quad (4)$$

where $D_l = l(l+1)C_l/2\pi$. Here, F_l , which we call the modal fraction (see Refs. [41, 42] for more details), measures the relative probability for a given angular mode over the full data set, playing a similar role to the probability of occurrence in a message of a letter belonging to a given alphabet in Shannon’s information entropy. Each data set is normalized to unity so that we can interpret F_l as a probability distribution. We use D_l to compute the \mathcal{D}_{JS} since it more clearly distinguishes the acoustic features.

The unbinned C_l computed from the temperature fluctuations observed by Planck can be found on the Planck Legacy Archive [43]; we use the third public release of the baseline high- l Planck TT power spectrum. (In future work, we plan to include polarization and temperature-polarization cross-correlation power spectra.) The cosmological Boltzmann code CAMB [44] is used to compute the angular power spectrum for a given model. The base set of cosmological parameters and their best-fit values as determined by the Planck 2018 analysis are summarized in Table I. All parameters except H_0 are left fixed at their best-fit values; H_0 is then set to be either 67.32 or 74.03 km/s/Mpc, the values reported by Planck 2018 (hereafter P18) and Riess, *et al.* 2019 (hereafter R19) [14], respectively.

Parameter	Best Fit
H_0 (km/s/Mpc)	67.32
$\Omega_c h^2$	0.12011
$\Omega_b h^2$	0.022383
τ	0.0543
$\ln(10^{10} A_s)$	3.0448
n_s	0.96605

TABLE I. Planck 2018 best-fit parameter values [8]. Future work will allow all of these parameters to vary. Note that H_0 is an inferred value from the fitted $100\Theta_*$; they may be used interchangeably in the base parameter set.

For each H_0 , we allow the DE equation of state to vary in the linear parametrization $w = w_0 + w_a(1 - a)$.

The distance, in terms of the \mathcal{D}_{JS} , from each model to the Planck data can be summarized by two surfaces: $\mathcal{D}_{\text{JS}}(w_0, w_a | h = 0.6732)$ and $\mathcal{D}_{\text{JS}}(w_0, w_a | h = 0.7403)$. Our goal here is not to determine which value of H_0 is the “correct” one, but to investigate whether a model with a modified DE equation of state can shift the inferred H_0 closer to R19. Such a model would have a shorter distance (in the sense of the \mathcal{D}_{JS}) to the Planck data and provide an alternative method of parameter estimation. A forthcoming full analysis will allow H_0 to vary along with the other parameters in Table I.

RESULTS

Figure 2 shows the \mathcal{D}_{JS} as a function of w_0 and w_a for both the P18 (right surface) and R19 (left surface) values of H_0 . Both surfaces display a valley running along a degenerate minimum curve where $\mathcal{D}_{\text{JS}} \simeq 8.442 \times 10^{-4}$. Given the interpretation of \mathcal{D}_{JS} as a metric between the two distributions, its minimum represents the preferred parameter data set. On the $H_0 = 67.32$ surface, the ΛCDM model is identified with a larger blue point. Figure 3 shows the degenerate curves along the \mathcal{D}_{JS} valley projected onto the (w_0, w_a) plane and fitted with a second-order polynomial. The dashed lines represent the error of the \mathcal{D}_{JS} minima, produced using the high and low errors in the measured values of the CMB TT acoustic power spectrum. Since the errors for each value of H_0 are small, the two curves are clearly distinguishable and do not overlap. Therefore, once one of the two parameters in the DE equation of state for this model is known, this approach allows for the determination of the other, thus breaking the degeneracy in a predictive way. In future work, we plan to apply a modified Fisher information matrix approach, adapted to \mathcal{D}_{JS} used here and applicable to many variables, in order to address the issue of correlated data points and potential errors in parameter prediction. In the Appendix, we sketch the initial steps toward this formalism for a single variable.

We also consider that data for the Hubble parameter as a function of redshift, $H(z)$ —along with the BAO volume-averaged effective distance ratio $D_V(z)/r_s(z_{\text{dec}})$ —could break the degeneracy in this model space compared to using the CMB data only. While in future work we will include these data sets *a priori* in the minimization of the \mathcal{D}_{JS} for a model, we use them here to examine their effect on the degeneracy found using only the Planck data. Taking pairs of values of w_0 and w_a along the degenerate curves, we use χ^2 to fit 38 measurements of $H(z)$, compiled from [45] and references therein, and 12 measurements of the BAO data, compiled from [35, 36]. The results for $\chi^2(w_0)$ for each H_0 and both data sets are shown in Fig. 4.

We find that including the additional late-time data sets does not reduce the degeneracy in a clear way. Table II reports the values of w_0 and w_a that minimize the

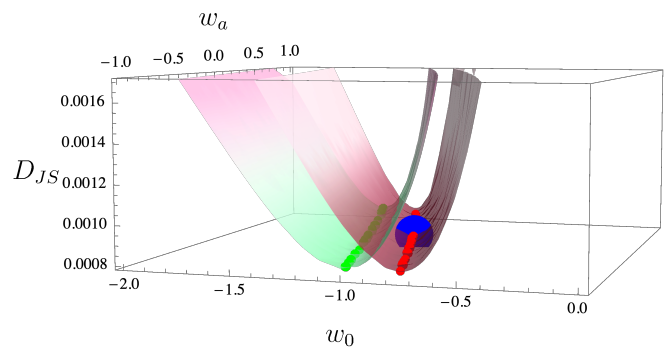


FIG. 2. \mathcal{D}_{JS} surfaces for ΛCDM and R19 values of H_0 in red and green, respectively. w_0 and w_a have been allowed to vary, but the other parameters were fixed at their best-fit values from Planck 2018 (see Table I). The red and green lines denote degeneracy in the model space; their distance from the Planck data is very nearly the same. The blue dot represents the ΛCDM model.

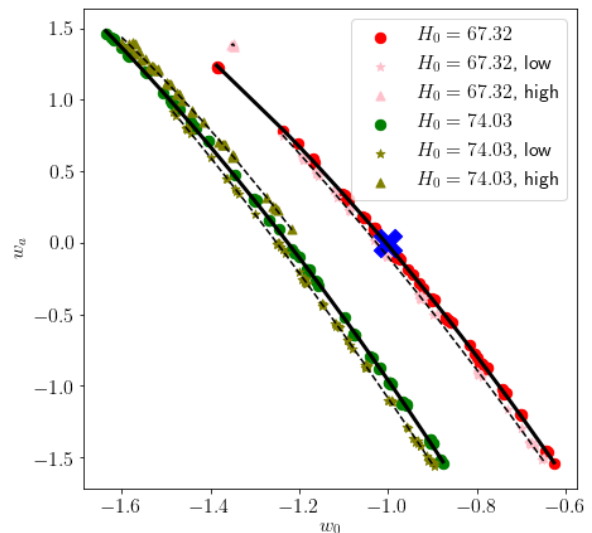


FIG. 3. Lines of degeneracy from Fig. 2 projected into the $w_0 - w_a$ plane and fit with a second-order polynomial, $w_a = c_0 w_0^2 + c_1 w_0 + c_2$. Here, $[c_0, c_1, c_2] = [-1.061, -5.792, -4.750]$ and $[-1.013, -6.518, -6.467]$ for P18 (right curve) and R19 (left curve) values of H_0 , respectively. The solid lines represent the best fit to the acoustic power spectrum of the CMB, while the dashed lines represent fits to the high and low errors of the the CMB acoustic power spectrum. The finite lengths of these lines indicate a finite $w_0 - w_a$ parameter space. The blue x represents the location of the ΛCDM model.

χ^2 for the BAO and $H(z)$ data, for both the P18 and R19 H_0 . Neither the BAO nor the $H(z)$ data show a significant difference between the χ^2 for each H_0 , indicating that the addition of these data sets would allow either H_0 value.

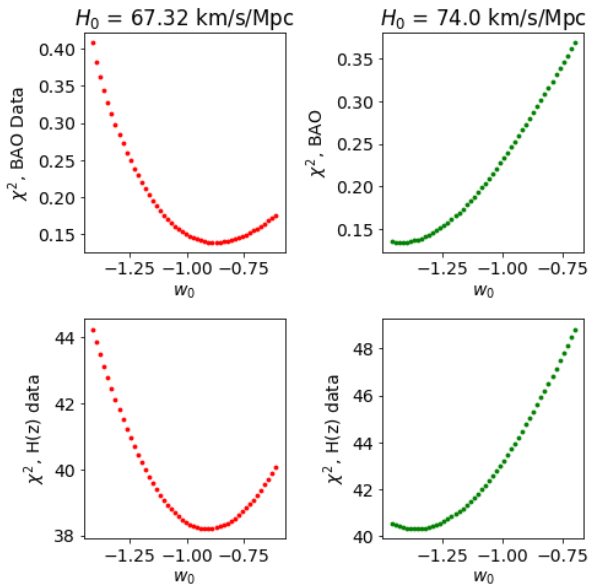


FIG. 4. For models along the curves of degeneracy found in Fig. 2, the χ^2 is plotted as a function of w_0 for (top) the model’s prediction of the BAO $D_V(z)/r_s(z_{\text{dec}})$ and the measured data, and (bottom) the model’s prediction for $H(z)$ and the measured data. The red and green curves come from using the P18 value and R19 value of H_0 , respectively.

Data	H_0 (km/s/Mpc)	w_0	w_a	χ^2
BAO	P18	-0.87	-0.51	0.139
BAO	R19	-1.41	0.73	0.134
$H(z)$	P18	-0.90	-0.38	38.2
$H(z)$	R19	-1.37	0.55	40.3

TABLE II. Values of w_0 and w_a along the curves of degeneracy from Fig. 2 that minimize the χ^2 to the BAO and $H(z)$ data sets.

CONCLUDING REMARKS

In this work, we introduced a new method to estimate cosmological parameters based on the Jensen-Shannon divergence \mathcal{D}_{JS} of information theory, inspired by the configurational entropy approach proposed in Ref. [41]. As a first application, we examined here the current tension in the value of the expansion rate H_0 , comparing the extended Λ CDM temperature anisotropy spectrum for models with dynamic DE parametrized in (w_0, w_a) space with the Planck 2018 temperature anisotropy data. For both values of H_0 , we found that there are curves of degeneracy in the (w_0, w_a) plane, characterized as nearly indistinguishable minima of the $\mathcal{D}_{\text{JS}}(w_0, w_a)$ surface. However, the two curves are along different values of the model parameter pair (w_0, w_a) , allowing for degeneracy breaking, indicating how our method could be used

for the potential resolution of the H_0 tension, once one of the two parameters is known. (We expect that similar degeneracy lines would be found using the Bayesian approach.) Extending our analysis to include $H(z)$ and BAO at different redshifts, we found that the extended data do not lift the degeneracy. Taking our limited parameter exploration of this work at face value, our results indicate that a possible resolution may indeed come from early-universe modifications of the standard cosmological model.

In a forthcoming paper, we plan to extend this analysis by running a MCMC to minimize the \mathcal{D}_{JS} in the full seven-parameter space, and to include data from BAO, $H(z)$, and the Planck polarization and temperature-polarization cross-correlation power spectra in our analysis. We expect this more complete approach to change the results plotted in Fig. 3, which should be considered our method’s first illustrative example. Our current results warrant further investigation of \mathcal{D}_{JS} as an alternative and transparent method of cosmological parameter estimation. A more complete study will allow us to directly compare parameter confidence intervals from our information-based analysis to others reported in the literature. Work along these lines is currently in progress.

ACKNOWLEDGMENTS

M.G. and M.S. were supported in part by a Department of Energy Grant No. DE-SC0010386 during the early stages of this collaboration, when M.S. was also supported by a Hull doctoral fellowship.

* Michelle.M.Stephens.GR@dartmouth.edu

† Sara.A.Vannah.GR@dartmouth.edu

‡ Marcelo.Gleiser@dartmouth.edu

- [1] Y. Akrami *et al.* (Planck Collaboration), Planck 2018 results I. Overview and the cosmological legacy of Planck, *Astron. Astrophys.* **641**, A1 (2020).
- [2] A. G. Sanchez *et al.*, The clustering of galaxies in the SDSS-III Baryon Oscillation Spectroscopic Survey: cosmological implications of the large-scale two-point correlation function, *Mon. Not. R. Astron. Soc.* **425**, 415 (2012).
- [3] M. Lopez-Corredoira, F. Melia, E. Lusso, and G. Risaliti, Cosmological test with the QSO Hubble diagram, *Int. J. Mod. Phys. D* **25**, 1650060 (2016).
- [4] W. L. Freedman, *Cosmology at a Crossroads*, *Nat. Astron.* **1**, 0121 (2017).
- [5] W. L. Freedman *et al.*, The Carnegie-Chicago Hubble Program. VIII. An Independent Determination of the Hubble Constant Based on the Tip of the Red Giant Branch, *Astrophys. J.*, **882**, (2019).
- [6] J. L. Bernal, L. Verde, and A. G. Riess, The trouble with H_0 , *J. Cosmol. Astropart. Phys.* 10 (2016) 019.
- [7] L. Verde, T. Treu, and A. G. Riess, *Nat. Astron.*, Tensions between the early and late Universe, **3**, (2019) 891.

- [8] N. Aghanim *et al.* (Planck Collaboration), Planck 2018 results. VI. Cosmological parameters, *Astron. Astrophys.* **641**, A6 (2020).
- [9] C. L. Bennett *et al.*, Nine-year Wilkinson Microwave Anisotropy Probe (WMAP) observations: Final maps and results, *Astrophys. J. Suppl. Ser.* **208**, 20 (2013).
- [10] M. Zaldarriaga, D. N. Spergel, and U. Seljak, Microwave Background Constraints on Cosmological Parameters, *Astrophys. J.* **488**, 1 (1997).
- [11] G. Efstathiou and J. R. Bond, Cosmic confusion: Degeneracies among cosmological parameters derived from measurements of microwave background anisotropies, *Mon. Not. R. Astron. Soc.* **304**, 75 (1999).
- [12] C. Howlett, A. Lewis, A. Hall, and A. Challinor, CMB power spectrum degeneracies in the era of precision cosmology, *J. Cosmol. Astropart. Phys.* **04** (2012) 027.
- [13] A. G. Riess *et al.*, A 2.4% Determination of the Local Value of the Hubble Constant, *Astrophys. J.* **826**, 56 (2016).
- [14] A. G. Riess, S. Casertano, W. Yuan, L. M. Macri, and D. Scolnic, Large Magellanic Cloud Cepheid Standards Provide a 1% Foundation for the Determination of the Hubble Constant and Stronger Evidence for Physics Beyond LambdaCDM, *Astrophys. J.* **876**, 85 (2019).
- [15] E. Di Valentino, A. Melchiorri, E. V. Linder, and J. Silk, Constraining Dark Energy Dynamics in Extended Parameter Space, *Phys. Rev. D* **96**, 023523 (2017).
- [16] S. Carneiro, P. C. de Holanda, C. Pigozzo, and F. Sobreira, Is the H_0 tension suggesting a 4th neutrino generation?, *Phys. Rev. D* **100**, 023505 (2019).
- [17] V. Poulin, K. K. Boddy, S. Bird, and M. Kamionkowski, Implications of an extended dark energy cosmology with massive neutrinos for cosmological tensions, *Phys. Rev. D* **97**, 123504 (2018).
- [18] V. Marra, L. Amendola, I. Sawicki, and W. Valkenburg, Cosmic variance and the measurement of the local Hubble parameter, *Phys. Rev. Lett.* **110**, 241305 (2013).
- [19] V. Poulin, T. L. Smith, T. Karwal and M. Kamionkowski, Early Dark Energy Can Resolve The Hubble Tension, *Phys. Rev. Lett.* **122**, 221301 (2019).
- [20] E. Di Valentino, E. V. Linder, and A. Melchiorri, Vacuum phase transition solves the H_0 tension, *Phys. Rev. D* **97**, 043528 (2018).
- [21] E. Di Valentino, A. Melchiorri, and O. Mena, Can interacting dark energy solve the H_0 tension?, *Phys. Rev. D* **96**, 043503 (2017).
- [22] K. Bolejko, Emerging spatial curvature can resolve the tension between high-redshift CMB and low-redshift distance ladder measurements of the Hubble constant, *Phys. Rev. D* **97**, no. 10, 103529 (2018).
- [23] E. Di Valentino, A. Melchiorri, and J. Silk, Beyond six parameters: extending Λ CDM, *Phys. Rev. D* **92**, 121302 (2015).
- [24] P. A. R. Ade *et al.* (Planck Collaboration), Planck 2013 results. XV. CMB power spectra and likelihood, *Astron. Astrophys.* **571**, A15 (2014).
- [25] M. Gerbino *et al.*, Likelihood Methods for CMB Experiments, *Front. in Phys.* **8**, 15 (2020).
- [26] T. Smith *et al.*, Early dark energy is not excluded by current large-scale structure data, arXiv:2009.10740v1.
- [27] R. Trotta, Bayes in the sky: Bayesian inference and model selection in cosmology, *Contemp. Phys.* **49**, 71 (2008).
- [28] J. R. Bond, G. Efstathiou and M. Tegmark, Forecasting cosmic parameter errors from microwave background anisotropy experiments, *Mon. Not. R. Astron. Soc.* **291**, L33 (1997).
- [29] M. White, D. Scott, and J. Silk, Anisotropies in the Cosmic Microwave Background, *Annu. Rev. Astrophys.* **32**, (1994).
- [30] A. Lewis and S. Bridle, Cosmological parameters from CMB and other data: A Monte Carlo approach, *Phys. Rev. D* **66**, 103511 (2002).
- [31] C. E. Shannon, A mathematical theory of communication, *Bell Syst. Tech. J.* **27**, 379 (1948).
- [32] S. Kullback and R. A. Leibler, On Information and Sufficiency, *Ann. Math. Stat.* **22**, 79 (1951).
- [33] J. Lin, Divergence measures based on the Shannon entropy, *IEEE Trans. Inf. Theory*, **37**, 145 (1991).
- [34] E. Aubourg *et al.*, Cosmological implications of baryon acoustic oscillation measurements, *Phys. Rev. D* **92**, 123516 (2015).
- [35] B. S. Haridasu, V. V. Luković, and N. Vittorio, Isotropic vs. Anisotropic components of BAO data: a tool for model selection, *JCAP* **1805**, no. 05, 033 (2018).
- [36] C. Cheng and Q. G. Huang, An accurate determination of the Hubble constant from Baryon Acoustic Oscillation datasets, *Sci. China Phys. Mech. Astron.* **58**, 599801 (2015).
- [37] M. Vargas-Magana *et al.*, Unraveling the Universe with DESI, arXiv:1901.01581.
- [38] M. Chevallier and D. Polarski, Accelerating universes with scaling dark matter, *Int. J. Mod. Phys. D* **10**, 213 (2001).
- [39] W. L. Freedman and B. F. Madore, The Hubble Constant, *Annu. Rev. Astron. Astrophys.* **48**, 673 (2010).
- [40] J. Q. Xia, H. Li, and X. Zhang, Dark Energy Constraints after Planck, *Phys. Rev. D* **88**, 063501 (2013).
- [41] M. Gleiser and N. Stamatopoulos, Entropic measure for localized energy configurations: Kinks, bounces, and bubbles, *Phys. Lett. B* **713**, 304 (2012).
- [42] M. Gleiser, M. Stephens, and D. Sowinski, Configurational entropy as a lifetime predictor and pattern discriminator for oscillons, *Phys. Rev. D* **97**, 096007 (2018).
- [43] Planck legacy archive, <http://pla.esac.esa.int/>.
- [44] A. Lewis, A. Challinor, and A. Lasenby, Efficient Computation of Cosmic Microwave Background Anisotropies in Closed Friedmann-Robertson-Walker Models, *Astrophys. J.* **538**, 473 (2000).
- [45] F. K. Anagnostopoulos and S. Basilakos, Constraining the dark energy models with $H(z)$ data: An approach independent of H_0 , *Phys. Rev. D* **97**, 063503 (2018).

APPENDIX
Error estimation using an adapted inverse Fisher
Information Matrix

Traditional model parameter estimation techniques use the inverse Fisher Information Matrix (FIM) to bound errors on the parameters from the Cramer-Rao inequality. We propose to adapt the FIM approach to our \mathcal{D}_{JS} approach. First, recall that for a set of M model parameters $\Lambda = (\lambda_1, \lambda_2, \dots, \lambda_M)$ and a likelihood function $L(x_a; \Lambda)$, where x_a is a data point belonging to a set of O observables $\mathcal{O} = (x_1, x_2, \dots, x_O)$, the $M \times M$ FIM is

$$\mathcal{F}_{\alpha\beta} = \left\langle \frac{\partial^2 \mathcal{L}}{\partial \lambda_\alpha \partial \lambda_\beta} \right\rangle, \quad (5)$$

where $\mathcal{L} \equiv -\ln L$. Simplifying to a single model parameter λ , the Fisher matrix \mathcal{F} is given by

$$\mathcal{F} = \frac{1}{2} \frac{\partial^2 \mathcal{L}}{\partial \lambda^2} \Big|_{\lambda=\bar{\lambda}}, \quad (6)$$

evaluated at the fiducial value $\bar{\lambda}$ (the best guess). We may evaluate similarly for $\mathcal{D}_{\text{JS}}(\lambda)$, by expanding about $\lambda - \bar{\lambda}$,

$$\mathcal{D}_{\text{JS}} \simeq \mathcal{D}_{\text{JS}}(\bar{\lambda}) + \frac{\partial \mathcal{D}_{\text{JS}}}{\partial \lambda} \Big|_{\lambda=\bar{\lambda}} (\lambda - \bar{\lambda}) + \frac{1}{2} \frac{\partial^2 \mathcal{D}_{\text{JS}}}{\partial \lambda^2} \Big|_{\lambda=\bar{\lambda}} (\lambda - \bar{\lambda})^2, \quad (7)$$

where we identify

$$\mathcal{F} \equiv \frac{1}{2} \frac{\partial^2 \mathcal{D}_{\text{JS}}}{\partial \lambda^2} \Big|_{\lambda=\bar{\lambda}}. \quad (8)$$

The zeroth-order term vanishes as does the first-order term, since the slope of the \mathcal{D}_{JS} curve at $\bar{\lambda}$ vanishes.

Using the definition of \mathcal{D}_{JS} in Equation 3, we write \mathcal{D}_{JS} as a function of the data, C_l^{obs} , and the parameter-dependent model spectrum $C_l(\lambda)$ as,

$$\begin{aligned} \mathcal{D}_{\text{JS}}(\{\lambda\}) = & -\frac{1}{2} \sum_l C_l^{\text{obs}} \ln \left(\frac{\frac{1}{2}(C_l^{\text{obs}} + C_l(\lambda))}{C_l^{\text{obs}}} \right) \\ & - \frac{1}{2} \sum_l C_l(\lambda) \ln \left(\frac{\frac{1}{2}(C_l^{\text{obs}} + C_l(\lambda))}{C_l(\lambda)} \right). \end{aligned} \quad (9)$$

Taking the derivatives we obtain,

$$\mathcal{F} = -\frac{1}{2} \sum_l \frac{\partial^2 C_l}{\partial \lambda^2} \log \left(\frac{\frac{1}{2}(C_l^{\text{obs}} + C_l)}{C_l} \right). \quad (10)$$

Generalizing to include many parameters $\{\lambda_\alpha\}$ gives

$$\mathcal{F}_{\alpha\beta} = -\frac{1}{2} \sum_l \frac{\partial^2 C_l}{\partial \lambda_\alpha \partial \lambda_\beta} \ln \left(\frac{\frac{1}{2}(C_l^{\text{obs}} + C_l)}{C_l} \right). \quad (11)$$

Since \mathcal{F} is a symmetric matrix, the 1σ error on the parameters is

$$\sigma_\alpha \geq \frac{1}{\sqrt{\frac{1}{2} \mathcal{F}_{\alpha\alpha}}}. \quad (12)$$